Desalination and Water Treatment
www.deswater.com

doi: 10.5004/dwt.2019.24184

158 (2019) 152–163
August

Cr(III) removal from tannery effluents using silica obtained from rice husk and modified silica

Moises Gutiérrez-Valtierra[a], Carmen Salazar-Hernández[b,*], Juan Manuel Mendoza-Miranda[b], Enrique Elorza-Rodríguez[a], María Jesús Puy-Alquiza[a], Martín Caudillo-González[a], Ma. Mercedes Salazar-Hernández[a,*]

[a]*Departamento de Ingeniería en Minas, Metalurgia y Geología de la Universidad de Guanajuato, Ex Hacienda San Matías S/N, Colonia San Javier Guanajuato, Gto. CP 36000, Mexico*
[b]*Unidad Profesional Interdisciplinaria de Ingeniería Campus Guanajuato, Instituto Politécnico Nacional (UPIIG-IPN), Av. Mineral de Valenciana No. 200 Col. Fracc. Industrial Puerto Interior, C.P. 36275 Silao de la Victoria, Guanajuato México, emails: merce@ugto.mx; msalazarh@ipn.mx*

Received 4 September 2018: Accepted 27 March 2019

ABSTRACT

Silica extracted from rice husk, which is represented as SRH, is inexpensive mesoporous silica useful for heavy metal removal from industrial waste effluents. SRH was synthesized through calcination at 650°C in an oxidant atmosphere obtaining a mesoporous silica with BET area of 297 $m^2 g^{-1}$ and 2.3 nm of pore diameter average, respectively. The surface of this silica was modified through a post-synthesis route with amine and polyamine groups obtained at 16% and 47% of modified surface with amine or polyamine groups (SRH–NH_2 and SRH–triamine). The chromium(III) removal capacity of SRH and amine-modified silica was tested with stock solutions, observing a fast sorption process and reaching its equilibrium adsorption time in 20 min. The resulting Cr(III) removal capacity was 6.7, 22.1 and 34.3 mg g^{-1} for SRH, SRH–NH_2 and SRH–triamine silicas, respectively. SRH and SRH amine silicas were used to remove Cr(III) from a sample taken from a tannery waste effluent from the city of Leon, Guanajuato, Mexico, and displayed a 70% and 90% removal, respectively. Our results confirm the ability of these inexpensive silicas to adsorb materials and their potential use in heavy metals removal processes from industrial waste effluents.

Keywords: Silica rice husk; Amine modified SRH; Cr(III) removal; Industrial waste effluents

1. Introduction

With the increase in awareness regarding the sustainable development in order to reduce the environmental pollution, the treatment of industrial waste effluents that contains heavy metals is an important issue in most of the industrial processes. Chromium is one of the most toxic heavy metals that cause serious pollution and harmful effects on human health. It can exist in trivalent (Cr(III)) and hexavalent (Cr(VI)) oxidation states. The common process of using Cr(III) for tanning in tannery industry is a major cause for high influx of Cr in the environment [1]. Tannery industry particularly use chromium sulfate for commercial practice due to its capacity to produce softer, weightless, bright-shale leathers with high wet heat resistance in short periods of time. The main methods to treat waste effluents that contain Cr(III) include adsorption, ionic exchange, reverse osmosis, biosorption, and reduction-chemical precipitation [2].

Adsorption is an effective method to remove heavy metals, therefore, the use of mesoporous silica (MS) and hybrid mesoporous silica (HMS) materials gained special

* Corresponding authors.

attention by its application in pre-concentration and removal of different heavy metals in aqueous systems, specially to remove Co(II), Cu(II), Cu(I), Pb(II), Cr(VI) and other ions [3–9]. However, these materials cannot be used in industrial waste effluent treatments due to the high cost of mesoporous silica precursor. Thus, silica precursors frequently used are alkoxysilane, tetraethoxysilane (TEOS) or tetramethoxysilane (METEOS) [10–13]. Consequently, in order to reduce the production costs of MS and HMS, some researchers used mixtures of TEOS-sodium silicate or sodium silicate as silica precursors. Textural properties of these materials are improved when silicate composition is moderate (below 30%) [14]. Alternatively, some researchers proposed the mesoporous silica hydrothermal synthesis from sodium silicate to obtain different morphologies, depending on the pH and template used [15–19].

Moreover, rice husk has been widely used as sorbent for heavy metals by its advantages such as the physicochemical properties (similar to adsorbent materials); average surface area of 272.5 $m^2 g^{-1}$, and a surface basicity at 0.45 meq mg^{-1}. The adsorbent capacity of the rice husk has been related to its chemical composition; this bio-adsorbent has a high content of carbon and silica [20]. Thus, the RH has been used to obtain activated carbon as adsorbent for contaminants removal such as dye, gasoline, methane and other [21–25]. For example, Masoud et al. [26] obtained activated carbon from calcination of the rice husk pretreated with KOH and HCl; observing an adsorption capacity for Fe(III) of 3.31 mg g^{-1}.

On the other hand, rice husk has become an excellent source from inexpensive silica [27–29]. For example, Hernández et al. [29] reported the extraction of mesoporous silica from rice husk with a surface area close to 286 $m^2 g^{-1}$ and an average porous diameter of 4.45 nm. Proposing, these silicas as an alternate system for drug delivery system. Mehdinia et al. [30] used the silica extracted from rice husk, represented as SRH, as an absorbent of heavy metals, reaching a 98% removal of Cr(VI) in 60 min in a 5 mg L^{-1} Cr(VI) for a synthetic solution. Moreover, Sivakumar [31] used SRH to remove Cr(VI) from tannery wastes and determined a 78.1 mg g^{-1} charge capacity.

Tannery wastes are complex systems with a high content of solids (grease and fur) that are commonly eliminated by flocculation processes. Furthermore, tannery wastes contain mainly trivalent chromium. Although, the toxicity of Cr(III) is lower that Cr(VI), its removal is necessary due to oxidation mechanisms and speciation leads to the formation of Cr(VI); which causes several health and environmental problems.

Thus, the aim of this work is to report the capacity of SRH and modified SRH with amine and triamine groups to remove Cr(III) from a tannery waste effluent from leather tannery located in the city of Leon Guanajuato, Mexico, analyzing the effect of the modifier and pH on Cr(III) capacity removal and the recycling capacity of SRH and modified SRH.

2. Experimental procedure

2.1. SRH synthesis

The SiO_2-rice husk was obtained according to the methodology reported by Hernández et al. [29], where 125 g of the rice husk were leached from a mixture of 140 mL HCl, 30 mL HNO_3 and 30 mL distilled water for 1 h. Then, the rice husk was washed with distilled water to remove the excess of acid. All organic materials were removed through thermal treatment at 600°C during 2 h in a Thermoscientific electric circular furnace F-21135 with a heating rate of 10°C min^{-1}.

2.2. Modified SRH synthesis

SRH was modified by post-synthesis methodology; the modifiers were aminopropyltrimethoxisilane, APTMS (99%, Sigma-Aldrich, México) and N^1-(3-trimethoxysilylpropyl) diethylendiamine, N-DEA (99%, Sigma-Aldrich, México). SRH was suspended in 150 mL of reactive grade ethanol (90%; MERCK, México) and the modifier was added according to proportions described in Table 1. NH_4OH (0.5 mL) was employed as condensation catalyst and the mixture was set to reflux with constant stirring for 24 h. Subsequently, the solid was recovered by filtration, washed with ethanol and dried at 90°C during 12 h.

2.3. Silica characterization

The SRH and modified SRH (SRH–NH_2, SRH–triamine) were characterized with FTIR spectroscopy using a Perkin Elmer spectrum 100 Analyzer in KBr pellets, measuring 400–4,000 cm^{-1}. Average of 32 scans with a 4 cm^{-1} resolution and FTIR analyses corroborated the silica modification. Additionally, the textural properties of samples were assessed via N_2 adsorption–desorption isotherms at 77 K in a Micromeritics ASAP-2010 instrument. Samples were degassed overnight at 180°C and 71 mm Hg prior to measurements. The surface area was calculated using the BET method, and the average pore diameter was calculated by applying the Barret, Joyner and Halenda (BJH) method to the desorption branch of the isotherm. Moreover, the zeta potential and isoelectric point were determined with a Zetasizer NanoZS Instrument from Malvern Co. Ltd., UK, equipped with a He-Ne laser; the samples were dispersed in KCl 1 mM. The variation of charge in silica surface for SRH-modified could be related with the adsorption mechanics and the different capacity of adsorption according to the pH solution.

On the other hand, the organic modifier was measured through thermogravimetric analysis (TGA), and ceramic yield was determined. TGA test was carried out in a temperature range of 25°C–1,000°C with a 120°C min^{-1} temperature rise using an oxidant atmosphere in a PerkinElmer Instrument SII Diamond TG/DTA Thermogravimetric/differential thermal analyzer. Additionally, the morphology of silicas was observed with a Jeol-6510 plus SEM microscope.

2.4. Adsorption study

The Cr(III) adsorption study was performed using Cr(III) stock solutions with a 30–500 mg L^{-1} concentration. These were fixed dissolving $CrOHSO_4$ $5H_2O$ powder (99%, Sigma-Aldrich, México) in deionized water. Adsorption experiments were carried out using a batch system at room temperature (25°C) with a 24 rpm constant stirring on the other hand,

Table 1
SRH and modifier molar percentages

SRH-modified	mmol		
	SRH	APTMS	N-DEA
SRH–NH_2	83.3	12.5	
SRH–triamine	166.7		30

pH was regulated with HCl solution, fixing the pH solution at: 1.5, 2.3 and 4, respectively. Cr(III) adsorption was not evaluated at pH > 4 due to the precipitation of chromium as $Cr(OH)_3$. A weighed mass of SRH, SRH–NH_2 and SRH–triamine (0.1 g) was added to Cr(III) stock solutions (10 mL) with different concentrations (30–500 mg Cr L^{-1}). Chromium was adsorbed by the silica and the residual was determined by atomic absorption using a PerkinElmer Analyst-200 spectrometer. Cr-residual readings were taken in 5 min intervals for 40 min.

The amount of Cr(III) adsorbed at time t (q_t) was calculated according to Eq. (1), where C_0 and C_t were the concentration at initial and at time t of Cr(III) in the solution (mg L^{-1}), m is the amount of adsorbent used (g) and V is the solution volume (L). The removal efficiency was calculated according to Eq. (2).

$$q_t = \frac{\left(C_0 - C_t\right)}{m} \times V \tag{1}$$

$$\text{Removal}\left(\%\right) = \frac{C_0 - C_e}{C_0} \times 100 \tag{2}$$

2.5. Cr(III) removal from the tannery effluent

Tannery waste effluents contain many suspended solids which must be removed before the Cr(III) adsorption process. The suspended solids were eliminated through flocculation with $FeCl_3$ at 1% and then the system was stirred during 30 min at 250 rpm to homogenize the flocculent in the solution. After 24 h, suspended solids were removed by filtration. The Cr(III) tannery solution free of suspended solids was used for the metal removing study using SRH and modified SRH. The adsorption process temperature was 25°C and different amounts of adsorbent silica were employed: 0.1, 0.2, 0.4, 0.6, 0.8, 1.0 and 2 g. Silica was added to 10 mL of Cr(III) tannery solution (2,000 mg L^{-1} Cr) and stirred for 20 min at 24 rpm. Subsequently, the residual chromium in the solution was determined by atomic absorption employing a PerkinElmer Analyst-200 atomic absorption spectrophotometer.

2.6. SRH and SRH-modified recycling performance

Recycling performance was determined for silica materials employed, Cr(III) solution stock at pH 4, pH corresponding to tannery waste effluents. Then, Cr(III) removal capacity was evaluated until five cycles of adsorption–desorption; chromium desorption was done using HCl 25% v solution.

3. Results and discussion

3.1. SRH and modified SRH characterization

Fig. 1 shows the FTIR characterization of SRH and modified SRH (SRH–NH_2 and SRH–triamine). SRH showed Si–O–Si broad signals at 1,090 cm^{-1} (ν_{as}), and 822 cm^{-1}(ν_s), water adsorption (3,456 cm^{-1} (ν) and 1,670 cm^{-1} (δ)) and Si–OH groups at 980 cm^{-1} [27]. Meanwhile, the amine group modified in the SRH–NH_2 and SRH–triamine shows the vibration νC–H at 2,945–2,862 cm^{-1} and δC–H at 1,400–1,385 cm^{-1}, these vibrations are the confirmation of the organic group in the silica matrix.

Fig. 2 shows the TGA analyses of SRH and modified silicas. SRH shows only one event of weight loss and it corresponds to physisorbide water in the silica (Signal 1 at 20°C–100°C). In contrast, modified silicas show two events of weight loss, physisorbide water (Signal 1 at 20°C–100°C)

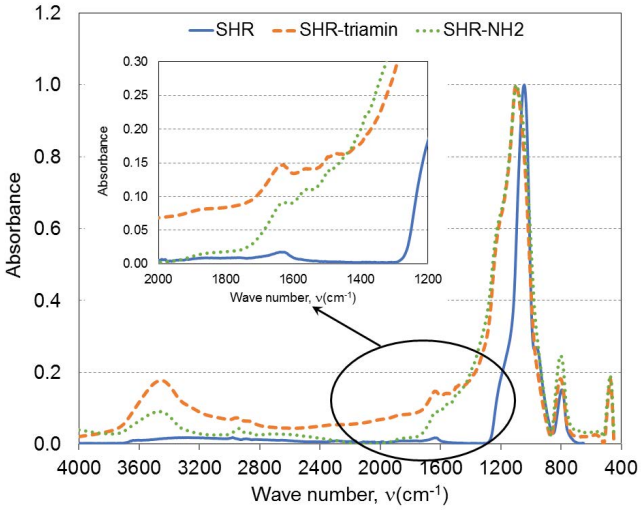

Fig. 1. SRH, SRH–NH_2 and SRH–triamine FTIR analysis.

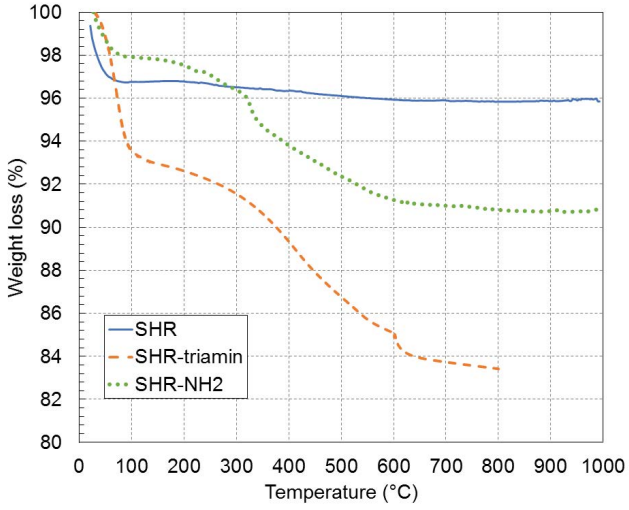

Fig. 2. TGA analysis of SRH, SRH–N_2 and SRH–triamine.

and the organic materials decomposition (Signal 2 at 195°C–600°C). Table 2 indicates the water percentage and organic material present in the silica and were calculated using the integral method. The ceramic yield is reported, as well.

According to data reported in Table 2, SRH is high ceramic yield silica (95.9%), only containing 6.87% of physisorbide water and no organic materials. On the other hand, the modified silica SRH–NH_2 contains a 29.8% of organic material, while SRH–triamine has 37.6%. Their ceramic yield decreases from 59.5% and 48.7%, respectively.

Textural properties of silicas are determined by nitrogen adsorption–desorption isotherms (Fig. 3a). All silicas show type IV isotherms, which are common characteristic of mesoporous materials. On the other hand, the H4 hysteresis loop indicated the formation of meso- and macropores in the silica. Fig. 3b concentrates BJH analyses displaying different pore distributions for silicas. SRH presented three pore sizes, one broad pore distribution at 1.7 nm and shoulders at 2.8 nm. The organic modifier produced changes to the surface structure originating a bi-modal pore distribution for SRH–NH_2, small and broad pore distribution at 2.4 nm and main pore distribution at 2.45 nm. Finally, triamine group (SRH–triamine) shows a broad mono modal pore distribution at 3.8 nm and changes in the pore distribution depending of the silica modifier added and its arrangement in the structure.

Table 3 shows the textural properties of all silicas. According to textural properties, the amine and triamine groups modified equally the surface area and volume pore; amine group decreased at 53.8% of A_{BET}, while the triamine group at 59.3%. However, due to the size of the modifying molecule, the pore size increases 11.54% for SRH–NH_2 and 51.17% for SRH–triamine. Similar textural properties suggest an equal adsorption capacity for both modified silicas.

On the other hand, silicas morphological characterizations were assessed by SEM (Fig. 4). SRH shows a rough morphology, similar to rice husks and fragmented particles (Fig. 4a), while modified silicas show the fragmentation of silica particles and the presence of smooth fibers as well (Figs. 4b and c).

Zeta potential for SRH and SRH-modified are shown in Fig. 5. The SRH has a large negative potential over a wide pH observing an isoelectric point (IEP) around 2.4, this behavior must be due to deprotonated silanol group on silica surface. While, the SRH–NH_2 and SRH–triamine show a positive surface as a function of pH. The positive charge in the surface of SRH–NH_2 is shown at 0–4.6 pH, observing the IEP at pH of 4.6, however, the SRH–triamine shows a positive surface in a wide range of the pH from 0 to 9, observing the IEP at a pH of 9.0.

Table 2
Percentage of modifier present in SRH

Silica	Percentage (%)		
	Water physisorbide	Organic material	Ceramic yield
SRH	6.87	0	95.94
SRH–NH_2	10.1	29.8	59.5
SRH–triamine	12.6	37.6	48.7

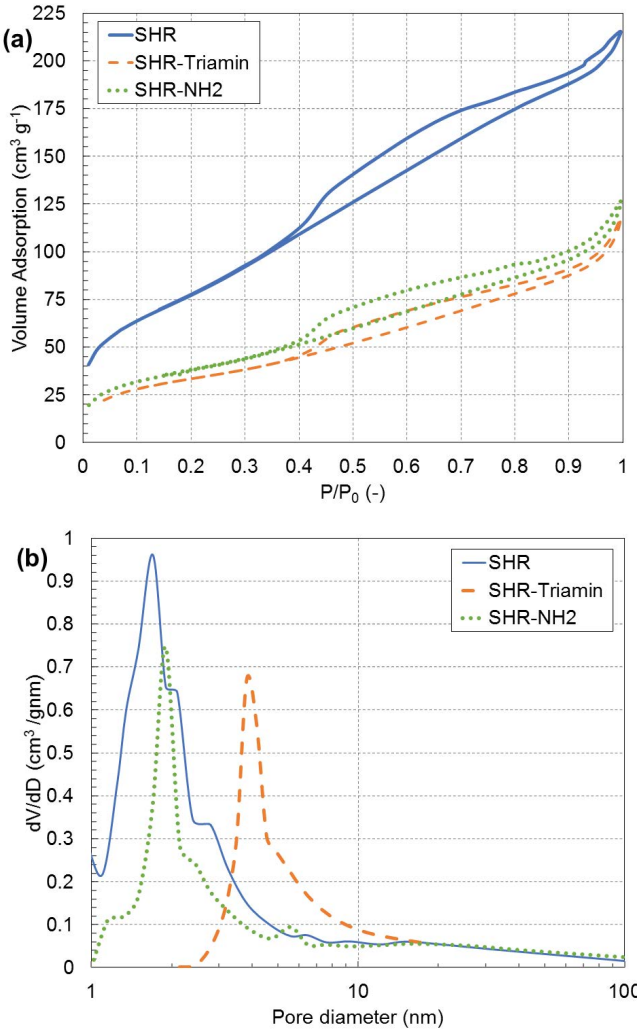

Fig. 3. (a) Nitrogen adsorption–desorption isotherm and (b) BJH porous distribution.

The charge changes on the surface of the silica by the presence of the amino and triethylene-amino groups suggesting a different mechanism of chromium adsorption in silicas; which will be discussed later.

3.2. Cr(III) adsorption using SRH and modified SRH

Fig. 6 shows the removal capacity of SRH, SRH–NH_2 and SRH–triamine in presence of different typical solutions of $CrSO_4OH$ (pH = 4), where the Cr(III) concentration varies between 443 and 100 mg L^{-1}. SRH shows a moderate efficiency; a 99% of Cr(III) in the solution with a low concentration (<140 mgL^{-1}) is adsorbed, and 42%–72% of the Cr(III) is absorbed for the solution with high concentration (443–227 mg L^{-1}). In contrast, modified rice husk silicas with amine and triamine groups show a higher efficiency, removing up to 99% of Cr(III) in both lower and higher concentration (443–100 mg L^{-1}). The adsorption equilibrium from SRH and SRH-modified was observed at 20 min.

Table 3
Textural properties of silica rice husks

	A_{BET} ($m^2\ g^{-1}$)	% Modified A_{BET}	Pore volume ($cm^3\ g^{-1}$)	% Modified pore volume	Pore diameter (nm)	% Modified pore diameter
SRH	297.3		0.35		2.3	
SRH–NH_2	137.2	53.85 (–)	0.18	48.57 (–)	2.6	11.54 (+)
SRH–triamine	120.8	59.36 (–)	0.152	56.6 (–)	4.71	51.17 (+)

(+) Indicates increase; (–) Indicates decrease.

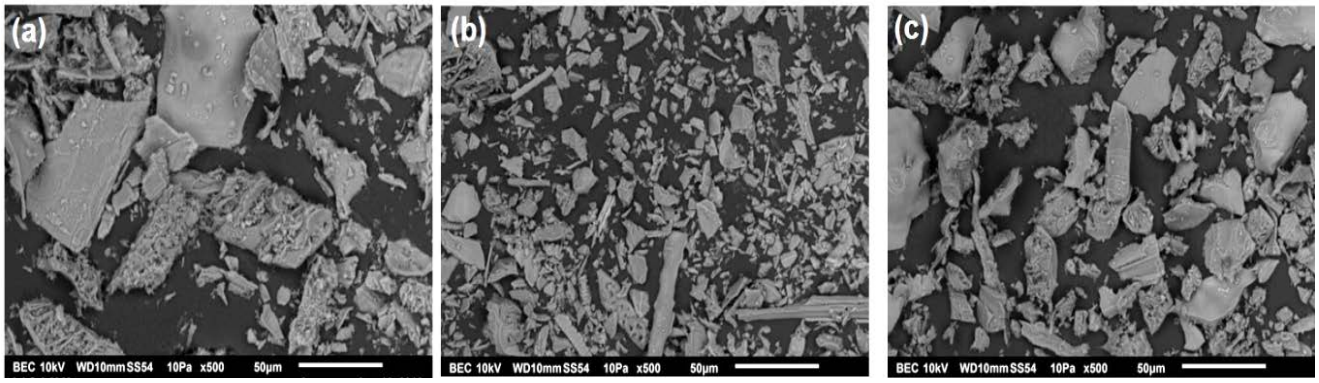

Fig. 4. SEM characterization of silicas: (a) SRH, (b) SRH–NH_2 and (c) SRH–triamine.

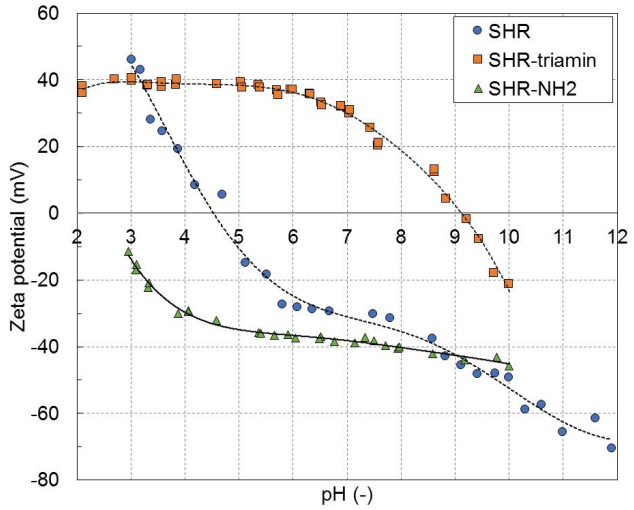

Fig. 5. Zeta potential of SRH and amine-modified SRH.

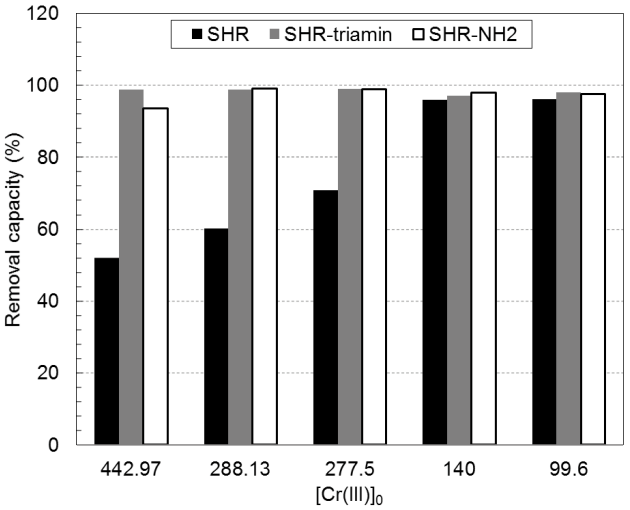

Fig. 6. Chromium removal capacity of silicas: SRH, SRH–NH_2 and SRH–triamine.

3.3. pH effect on Cr(III) adsorption using SRH and modified SRH

Fig. 7 shows the dependence of chromium adsorption on the pH of solution; the study was done with a solution of 288 mg L^{-1} of Cr(III). The SRH shows low adsorption capacity at pH less than 2 and moderate adsorption capacity at pH 4 (41%); Furthermore, the Cr(III) removal capacity of SRH-modified was around 99% using a pH of 2.3 and 4, while a moderate Cr(III) removal capacity was observed at pH of 1.5; SRH–NH_2 removes 53%, SRH–triamine removes 62% and SRH 2%, respectively.

The adsorption capacity for SRH and modified SRH depends of the charge on surface that controls the interactions with the sorbate. The SRH shows a negative zeta potential at pH of 1.5–4; suggesting that the Cr(III) adsorption takes place through the interaction between deprotonated silanol (SiO^-) and the positive charge of Cr^{3+} (Fig. 8a). At a pH below of 2, the SRH is closed to IEP, thus, Cr^{3+} adsorption is negligible.

On the other hand, zeta potential for SRH–NH_2 and SRH–triamine was positive at pH of 2–4; Masoud et al. [26]

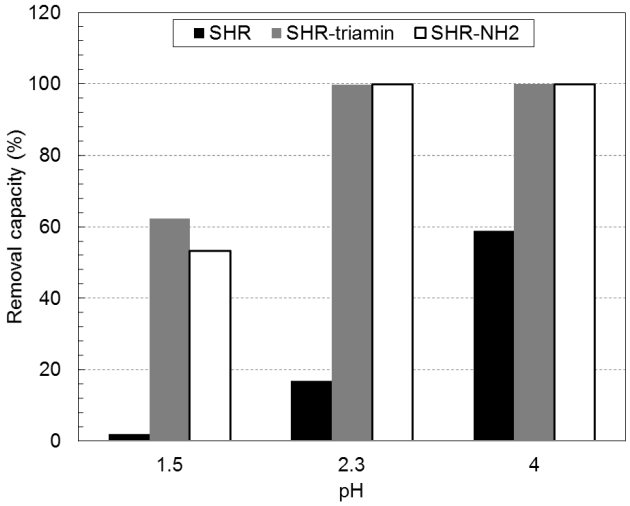

Fig. 7. pH effect in the capacity of silicas: SRH, SRH–NH_2 and SRH–triamine.

suggest that the adsorption of heavy metals on SRH is carried out by ion exchange mechanism, this mechanism suggests the chromium adsorption on amine-modified SRH (Fig. 8b). At pH below 2, a high positive surface ($\zeta > 40$ mV) was observed for SRH–NH_2 and SRH–triamine; this charge leads the repulsion interaction between chromium and amine groups diminishing the adsorption capacity.

3.4. Isotherm studies

The adsorption studies were evaluated by Langmuir, Freundlich and Temkin isotherm models [32–35]. The adsorption load as a normalized standard deviation, Δq, was calculated according to Eq. (3). The Δq quantitatively compares the applicability of different isotherm models to SRH adsorption system [35], where N is the number of data point, q_{exp} and q_{cal} (mg g^{-1}) are the experimental and calculated amount adsorbed of Cr(III) at equilibrium, respectively.

$$\Delta q(\%) = 100 \times \sqrt{\frac{\Sigma\left(\frac{q_{exp} - q_{cal}}{q_{exp}}\right)^2}{N-1}} \tag{3}$$

The Langmuir isotherm (Eq. (4)) evaluates the monolayer adsorption in the system, where q_e (mg g^{-1}) is the amount adsorbed at equilibrium, Q_0 (mg g^{-1}) is the maximum adsorption capacity and K_L (L mg^{-1}) is the Langmuir constant related to the energy of adsorption [35].

$$q_e = \frac{Q_0 K_L C_e}{1 + K_L C_e} \tag{4}$$

The Freundlich isotherm (Eq. (5)) represents at adsorption heterogeneous surface where the binding sites are not equivalent. Where q_e (mg g^{-1}) is the amount adsorbed at equilibrium, K_F is the Freundlich constant (mg/g $[L/mg]^{1/n}$) and $1/n$ is the measure of adsorption intensity, if $1/n < 1$ the adsorption is favorable and if $1/n > 1$ the adsorption is unfavorable [32,35].

$$q_e = K_F C_e^{1/n} \tag{5}$$

Meanwhile, Temkin isotherm assumes that the heat adsorption decreases linearly with the coverage due to adsorbent–adsorbent interaction (Eq. (6)) [30,33] where A (L g^{-1}) is the Temkin constant, b (J mol^{-1}) is the constant related to sorption heat, R is the gas constant (8.314 J mol^{-1} K^{-1}) and T is the absolute temperature.

$$q_e = B \ln A + B \ln C_e \tag{6}$$

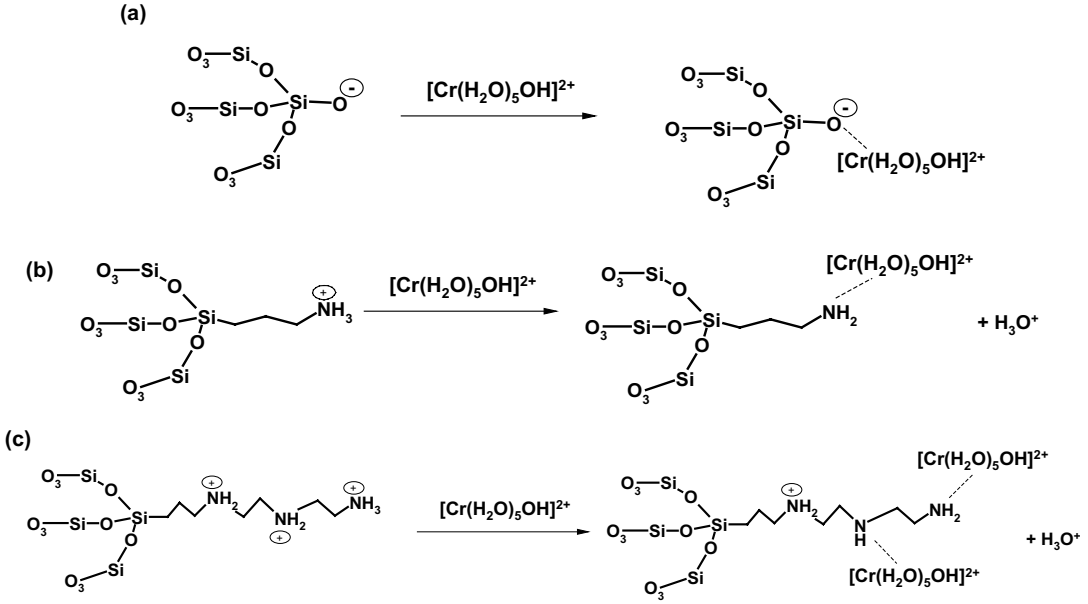

Fig. 8. Adsorption of Cr(III) on SRH (a), SRH–NH_2 (b) and SRH–triamine (c).

$$B = \frac{RT}{b} \tag{7}$$

Fig. 9 shows the isotherm of adsorption of Cr(III) using SRH and modified SRH (SRH–NH_2, SRH–triamine) and the adjusted of the experimental data to Langmuir, Freundlich and Temkin isotherm models, the R^2 from the experimental data with these isotherm models are lying between 0.92 and 0.99. Tables 4–6 show the parameters of the adsorption isotherm and the Δq for the experimental data. Langmuir isotherm (Table 4) indicates a good fit of the experimental data, observing an R^2 of 0.9603–0.9964 and low standard deviation (around 2%). According to the isotherm model adsorption, the SRH shows moderate Q_0 of 25.2 mg g^{-1} compared with that reported by Sivakumar [31] of 78.1 mg g^{-1}, however, the modified silica shows a high removal capacity for Cr(III), the Q_0 increases to 45.45 and 204.1 mg g^{-1} for SRH–NH_2 and SRH–triamine, respectively. These results suggest that the amine groups in the modified silica rice husk improve the adsorption capacity of the SRH as a result of the coordination capacity of the amine groups with the chromium ions. The Gibbs energy for absorption process was calculated by Eq. (8); observing an exothermic adsorption with values around –26.04 at –19.55 kJ mol^{-1} (Table 4). The lower Gibbs energy value was determinate for modified SRH suggesting that the chromium ion chelation on modifier silica surface is an endothermic process, producing favorable conditions in the polyamine silica (SRH–triamine).

$$\Delta G = -RT \ln K_L \tag{8}$$

The separation factor (R_L) indicates if the adsorption process is favorable or unfavorable, it is calculated by Eq. (9), where C_0 is the initial concentration in mg L^{-1} and K_L is the Langmuir constant. The value of R_L lies between 0 and 1 indicating that the adsorption is favorable, while R_L greater than 1 represents unfavorable adsorption and R_L = 1 represents linear adsorption, while the adsorption process is irreversible if R_L = 0 [36]. Fig. 10 shows the R_L from chromium adsorption studies with values between 0.003–0.014, 0.008–0.034 and 0.04–0.14 for SRH, SRH–NH_2 and SRH–triamine, respectively, suggesting a favorable adsorption.

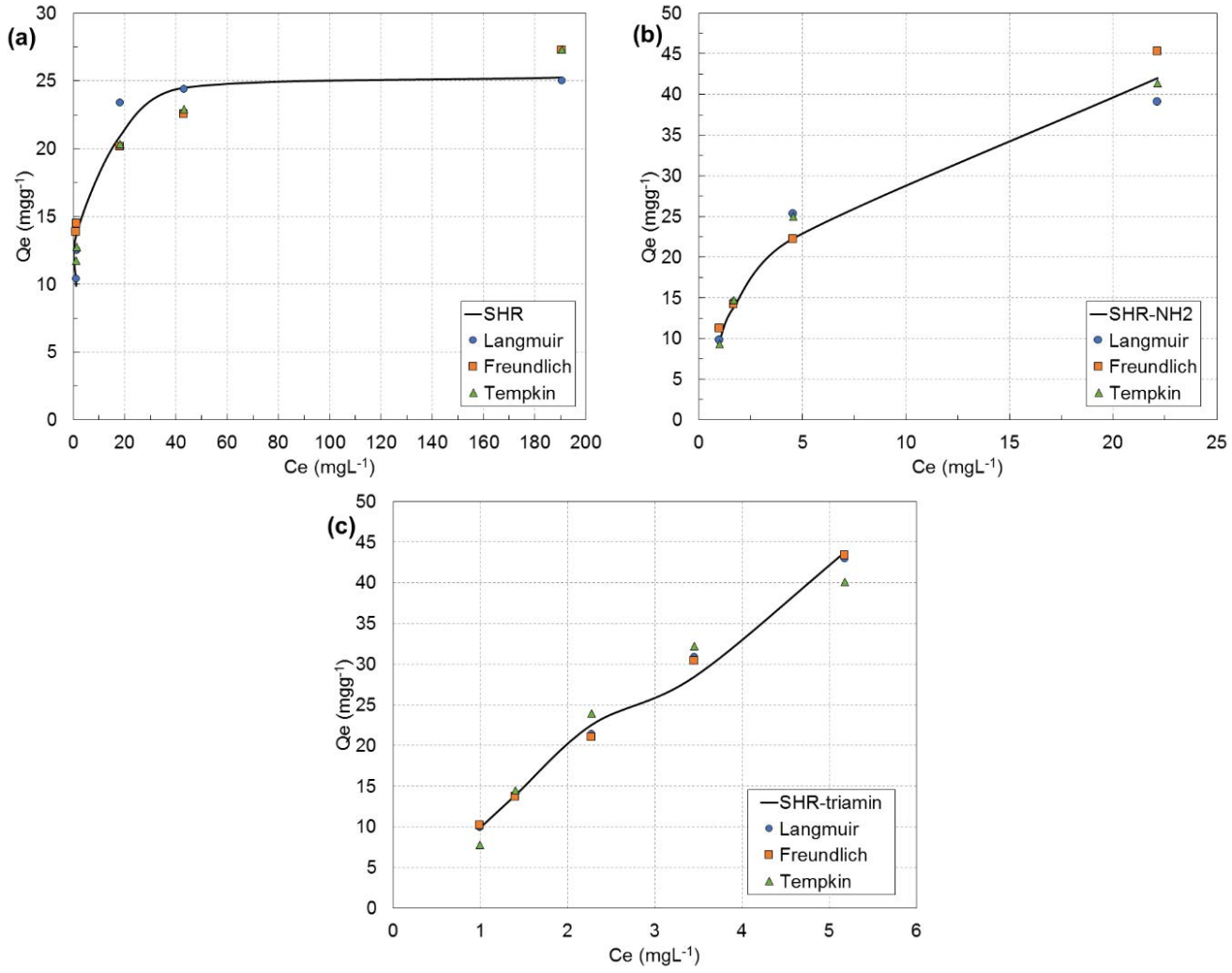

Fig. 9. Equilibrium isotherms for the removal of Cr(III) onto SRH (a), SRH–NH_2 (b) and SRH-triamine (c).

Table 4
Values of Langmuir isotherm constants for Cr(III) adsorption onto SRH, SRH–NH_2 and SRH–triamine

	Langmuir				
	Q_0 (mg g^{-1})	K_L (L mg^{-1})	R^2	Δq (%)	ΔG (kJ mol^{-1})
SRH	25.19	0.705	0.9603	1.99	–26.04
SRH–NH_2	45.45	0.275	0.9808	1.21	–23.70
SRH–triamine	204.082	0.0515	0.9964	2.56	–19.55

Table 5
Values of Freundlich isotherm constants for Cr(III) adsorption using SRH, SRH–NH_2 and SRH–triamine

	Freundlich			
	K_F ([mg/g]/[mg/L])$^{1/n}$	$1/n$	R^2	Δq (%)
SRH	13.85	0.1291	0.9258	4.57
SRH–NH_2	11.23	0.4499	0.9401	1.31
SRH–triamine	10.19	0.8799	0.9927	3.14

Table 6
Values of Temkin isotherm constants for Cr(III) adsorption using SRH, SRH–NH_2 and SRH–triamine

	Temkin			
	b (kJ mol^{-1})	A (L g^{-1})	R^2	Δq (%)
SRH	0.852	57.16	0.9361	3.14
SRH–NH_2	0.239	2.47	0.9769	2.54
SRH–triamine	0.126	1.49	0.9525	3.77

$$R_L = \frac{1}{1 + K_L C_0} \tag{9}$$

According to Freundlich isotherm, the Cr(III) adsorption on SRH and modified SRH is a favorable adsorption process, $1/n < 1$ (Table 5). Moreover, Temkin model shows that the heat adsorption (b) decreases with the amine modification in the surface (Table 6).

Consistent with adsorption isotherm models, the amine groups on SRH increase favorably the Cr(III) absorption. Therefore, these materials could be employed to remove this heavy metal in tannery waste effluents with high Cr(III) concentration becoming a major environmental hazard.

3.5. Cr(III) adsorption kinetic studies for stock solutions

The adsorption rate was analyzed using the semi-empirical pseudo-first and second-order kinetic model and the intraparticle diffusion; Table 7 summarizes the kinetic model and its parameters [32–35]. The adjustment of the experimental data at the kinetic model is summarized in Table 8, the pseudo-first kinetic model is not adjusted by the system; however, the adsorption rate is adjusted by the pseudo-second-order model.

The silica's maximum chromium adsorption capacity was measured using 0.5 g of silica materials and 20 mL of a Cr(III) solution at 5,200 ppm. The process adsorption time was 20 min and the system was stirred at 24 rpm. Table 9 includes all load capacity results, where SRH shows a lower load capacity (6.7 mg g^{-1}). In contrast, modified SRH values were 22.1 and 34.3 mg g^{-1} for SRH–NH_2 and SRH–triamine, respectively. These results suggest that the presence of amino groups in silica increase the chromium adsorption.

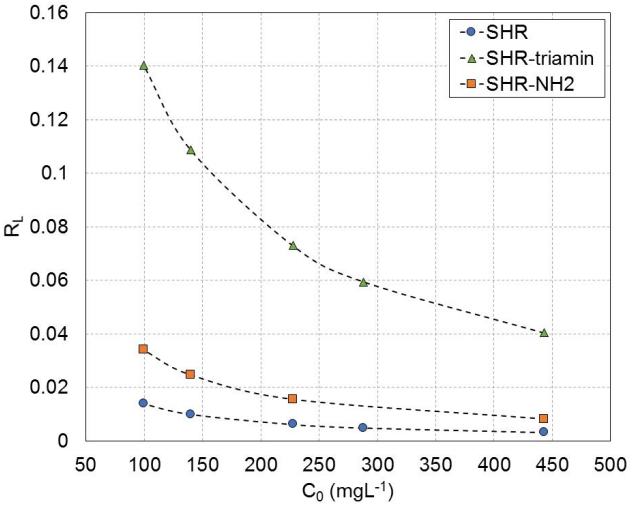

Fig. 10. R_L from the removal of Cr(III) onto (a) SRH, (b) SRH–NH_2 and (c) SRH–triamine.

Fig. 11 shows the concentration distribution of Si (adsorbent matrix) and Cr(III), obtained with EDS analyses in all silica's after the adsorption process. These micrographs show a high distribution of chromium on the materials surface (SRH, SRH–NH_2 and SRH–triamine); suggesting homogenous adsorption in all cases.

3.6. Cr(III) adsorption kinetic using tannery waste effluents

Table 10 shows the Cr(III) tannery solution characterization from Leon, Guanajuato, Mexico. The sample shows a high concentration of sediments and suspended solids as well as a high chromium concentration, around 2,177 mg L^{-1}. The removal of suspended solids was performed with $FeCl_3$-cationic flocculants using 1% by volume solution, before the adsorption study with both the SRH and modified SRH.

For the adsorption study, 20 mL of Cr(III) tannery solution free of suspended solids with a chromium concentration of 2,177 mg L^{-1} was employed. The adsorption process was performed with different amounts of SRH and modified SRH (0.2–2 g) (Fig. 12). The adsorption equilibrium time in

Table 7
Kinetic models

	Equation	Linear equation	Parameter
Pseudo-first-order	$\frac{dq_t}{dt} = K_1(q_e - q_t)$	$\log(q_e - q_t) = loge_e - \frac{K_1}{2.303} \times t$	K_1 rate constant (min^{-1}) q_e (mg g^{-1}) q_t (mg g^{-1})
Pseudo-second-order	$\frac{dq_t}{dt} = K_e(q_e - q_t)^2$	$\frac{t}{q_t} = \frac{1}{K_2 q_e^2} + \frac{t}{q_e}$	K_2 rate constant (g mg^{-1} min^{-1}) q_e (mg g^{-1}) q_t (mg g^{-1})
Intraparticle Diffusion	$q_t = f(t^{0.5})$	$q_t = K_i t^{1/2} + C$	K_i intraparticle diffusion constant (mg g^{-1} $min^{0.5}$) q_t (mg g^{-1})

Table 8
Kinetic constant for Cr(III) absorption on SRH and modified SRH

		SRH			SRH–NH_2			SRH–triamine		
	C_0 (mg L^{-1})	99.6	140	443.97	99.6	140	443.97	99.6	140	443.97
Pseudo-first-order	$Q_{e,exp}$	9.86	13.86	25.25	9.86	13.86	42	9.86	13.86	43.78
	$Q_{e,cal}$	6.42	9.5	20.94	9.78	13.823	40.3	9.85	13.85	43.77
	K_1 (min^{-1})	0.15	0.163	0.0359	0.854	1.03	0.254	0.854	0.966	1.09
	R^2	0.944	0.947	0.9742	1	1	0.999	1	1	1
	Δq (%)	12.33	11.12	1.03	0.331	0.003	1.81	0.0006	0.029	0.008
Pseudo-second-order	$Q_{e,exp}$	9.86	13.86	25.25	9.86	13.86	42	99.6	13.86	43.78
	$Q_{e,cal}$	10.02	13.75	25.91	9.73	13.75	42.55	9.73	13.75	43.78
	K_2 (g mg^{-1} min^{-1})	0.104	0.096	0.011	5.03	6.61	0.0324	5.03	6.61	0.529
	R^2	0.999	0.999	0.992	1	1	0.999	1	1	1
	Δq (%)	0.896	0.281	0.924	0.538	0.221	0.463	0.54	0.324	0.242
Intraparticle diffusion	K_i (mg g^{-1} $min^{-0.5}$)	0.754	1.06	4.79	6.15	0.0036	4.97	2.15	0.0043	0.0163
	R^2	0.9869	0.9869	0.9995	0.811	1	0.8907	0.8983	0.994	0.9834

Table 9
Adsorption capacity for SRH and modified SRH

	SRH	SRH–NH_2	SRH–triamine
Q (mg g^{-1})	6.7	22.1	34.3

Table 10
Tannery solution characterization

	Tannery Solution
pH	3.8
Conductivity (S/cm)	221
Sedimentation solid (mL/L)	82
Suspended solid (ppm)	114,500
Cr(III) (ppm)	2,177

all cases was 20 min. SRH shows a few Cr(III) adsorption capacity at lower dosages (0.2 and 0.4 g), then, when the dosage increases to 0.6 g, the removal percentage increases up to 52%, furthermore, when 2 g of SRH were added to the solution, the removal percentage increases up to 70%.

On the other hand, modified SRH shows high Cr(III) adsorption capacity in all dosages used (0.2–2 g). The removal capacity increased progressively in relation to the amount of silica added to the solution. SRH–NH_2 shows a 50% removal with 0.2 g of silica, and increases linearly up to 95% at 2 g. Additionally, SRH–triamine present an elevated Cr(III) adsorption capacity with dosages as low as 0.2 g, with a 60% adsorption and kept increasing to 99% when 2 g were added.

These results indicate that amine groups enhance Cr(III) adsorption in SRH because they allow the chelation of metals. Additionally, SRH–triamine shows an even higher Cr(III) adsorption capacity given the presence of a modified group with three nitrogen atoms, corroborated by the drastic increase in the adsorption capacity.

3.7. Recycling performance of SRH and SRH-modified in the Cr(III) adsorption

Fig. 13 shows the adsorption–desorption cycles for all tested silica observing its ability to recycle; the desorption in all cases was observed quantitatively using a solution of HCl

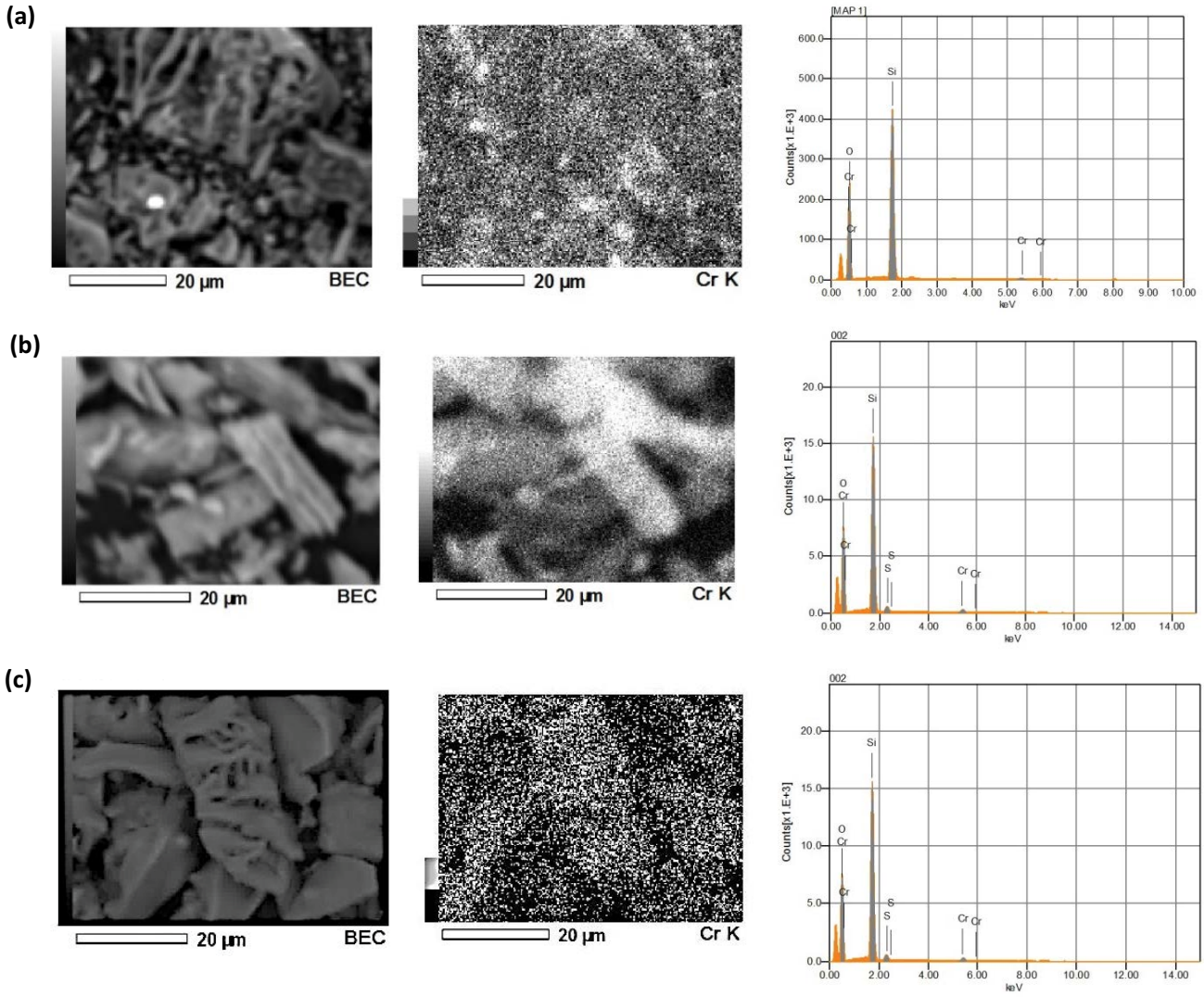

Fig. 11. EDS analyses showing the concentration distribution of Si and Cr in (a) SRH, (b) SRH–NH_2 and (c) SRH–triamine.

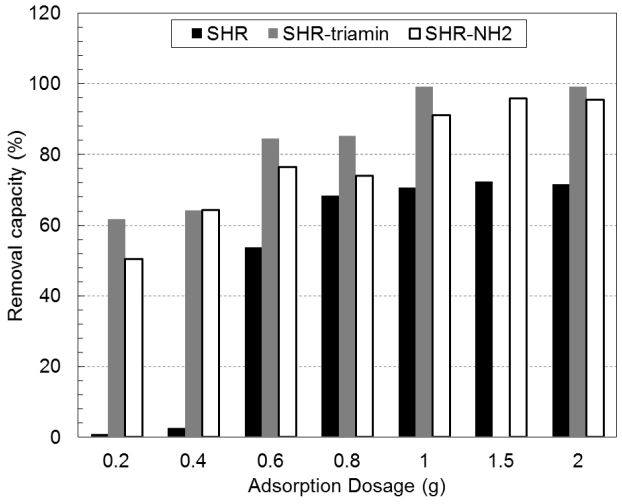

Fig. 12. Effect of adsorption dosage on Cr(III) removal in a tannery industry wastewater.

at 25%. SRH shows a moderate adsorption capacity up to two cycles, and negligible adsorption from third to fifth cycles. Second, SRH–NH_2 and SRH–triamine show high adsorption capacity in all cycle studies and quantitative desorption; these results suggest the feasible use of these silicas in Cr(III) removal from tannery effluent.

4. Conclusions

The SRH is an inexpensive silica with good adsorption properties. It shows high yield chromium removal capacity in both synthetic and tannery waste solutions. SRH exhibits a load capacity of 5.6 mg g^{-1} of chromium and a removal capacity of 70% in a tannery waste solution with a chromium concentration of 1,730 ppm. This capacity can be increased modifying the silica surface with amine and polyamine groups, resulting in a 22.1 and 34.3 mg g^{-1} load capacity for SRH–NH_2 and SRH–triamine, respectively. The chromium removal capacity for this silica in tannery waste solution can be 90%. Our results show the feasibility of the

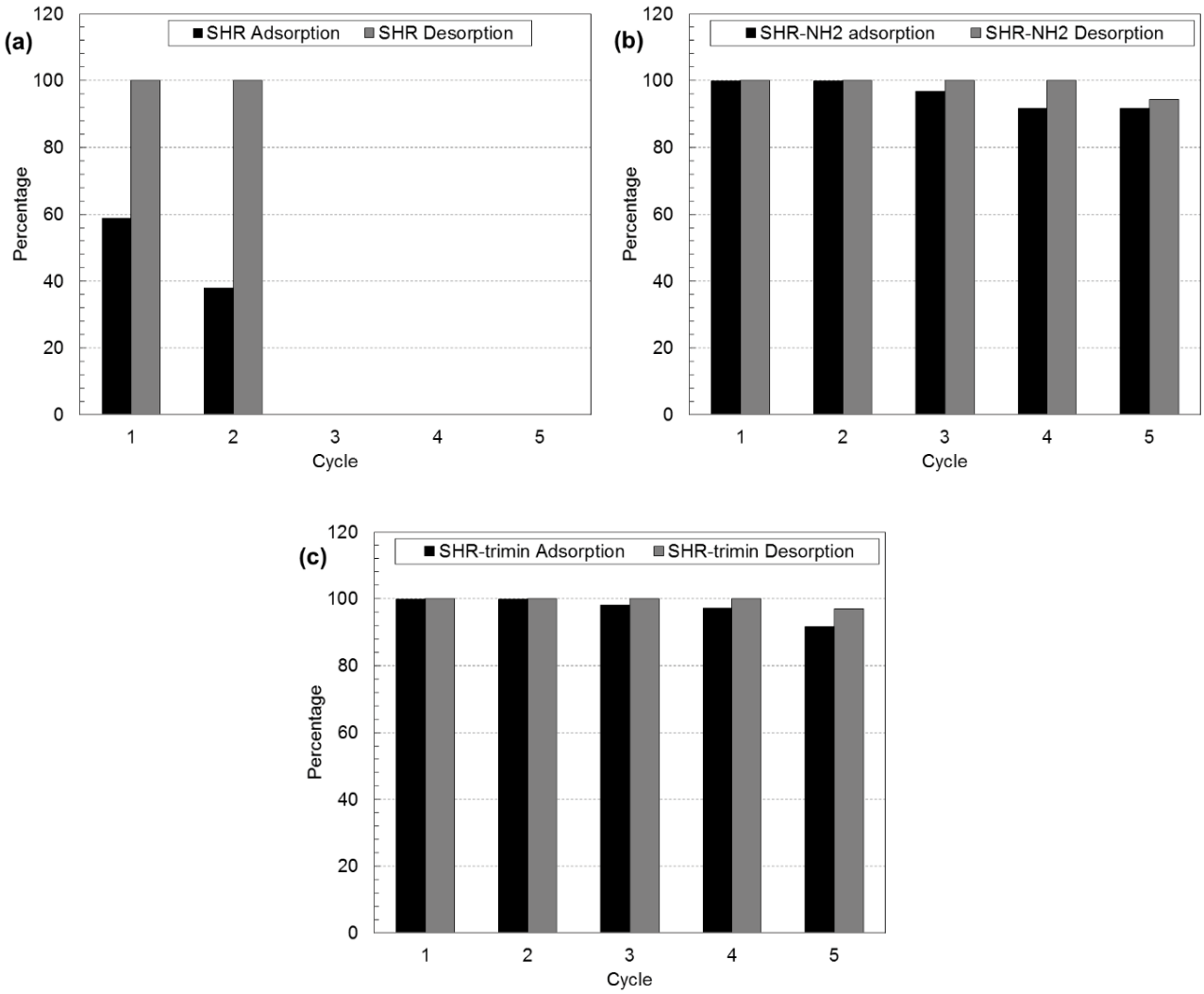

Fig. 13. Adsorption–desorption cycles for Cr(III) in: (a) SRH, (b) SRH–NH_2 and (c) SRH–triamine.

use of inexpensive materials such as SRH, SRH–NH_2 and SRH–triamine for heavy metals removal, such as Cr, found in industrial waste effluents, with a high chromium adsorption capacity recycling cycles.

Acknowledgements

The authors wish to acknowledge the financial support of the CONACyT through grant CB-257100/2015 and Guanajuato University through grant 19/2018. Also to Guanajuato University and LICAM-LAB of UG for the technical support in the analytical and SEM analysis.

References

[1] I.Y. El-Sherif, S. Tolani, K. Ofosu, O.A. Mohamed, A.K. Wanekaya, Polymeric nanofibers for the removal of Cr(III) from tannery waste water, J. Environ. Manage., 129 (2013) 410–413.
[2] M. Fabbricino, B. Naviglio, G. Tortora, L. d'Antonio, An environmental friendly cycle for Cr(III) removal and recovery from tannery wastewater, J. Environ. Manage., 17 (2013) 1–6.
[3] S. Parambadath, A. Mathew, M.J. Barnabas, S.Y. Kim, C.-S. Ha, Concentration-dependant selective removal of Cr(III), Pb(II) and Zn(II) from aqueous mixtures using 5-methyl-2-thiophenecarboxaldehyde Schiff base-immobilised SBA-15, J. Sol-Gel Sci. Technol., 79 (2016) 426–439.
[4] X. Huang, Y. Wang, X. Liao, B. Shi, Adsorptive recovery of Au^{3+} from aqueous solutions using bayberry tannin-immobilized mesoporous silica, J. Hazard. Mater., 183 (2010) 793–798.
[5] S. Isabel, P.-Q. Damián, Heavy metal complexation on hybrid mesoporous silicas: an approach to analytical applications, Chem. Soc. Rev., 42 (2013) 3792–3807.
[6] P.K. Jal, S. Patel, B.K. Mishra, Chemical modification of silica surface by immobilization of functional groups for extractive concentration of metal ions, Talanta, 62 (2004) 1005–1028.
[7] N. Zaitseva, V. Zaitsev, A. Walcarius, Chromium(VI) removal via reduction–sorption on bi-functional silica adsorbents, J. Hazard. Mater., 250–251 (2013) 454–461.
[8] M.K. Dinker, P.S. Kulkarni, Recent advances in silica-based materials for the removal of hexavalent chromium: a review, J. Chem. Eng. Data, 60 (2015) 2521–2540.
[9] Ma.M. Salazar-Hernández, C. Salazar-Hernández, E. Elorza-Rodríguez, H. Juarez Ríos, The use of mesoporous silica in the removal of Cu(I) from the cyanidation process, J. Mater. Sci., 50 (2015) 439–446.
[10] N.D. Petkovich, A. Stein, Controlling macro- and mesostructures with hierarchical porosity through combined hard and soft templating, Chem. Soc. Rev., 42 (2013) 3721–3739.

[11] C.T. Kresge, W.J. Roth, The discovery of mesoporous molecular sieves from the twenty year perspective, Chem. Soc. Rev., 42 (2013) 3663–3670.
[12] Z.-A. Qiao, L. Zhang, M. Guo, Y. Liu, Q. Huo, Synthesis of mesoporous silica nanoparticles via controlled hydrolysis and condensation of silicon alkoxide, Chem. Mater., 21 (2009) 3823–3829.
[13] B.G. Trewyn, I.I. Slowing, S. Giri, H.-T. Chen, V.S.-Y. Lin, Synthesis and functionalization of a mesoporous silica nanoparticle based on the sol–gel process and applications in controlled release, Acc. Chem. Res., 40 (2007) 846–853.
[14] J. Liu, Q. Yang, X.S. Zhao, L. Zhang, Pore size control of mesoporous silicas from mixtures of sodium silicate and TEOS, Microporous Mesoporous Mater., 106 (2007) 62–67.
[15] L. Sierra, J.-L. Guth, Synthesis of mesoporous silica with tunable pore size from sodium silicate solutions and a polyethylene oxide surfactant, Microporous Mesoporous Mater., 27 (1999) 243–253.
[16] K.-Z. Hossain, A. Sayari, Synthesis of onion-like mesoporous silica from sodium silicate in the presence of α,ω-diamine surfactant, Microporous Mesoporous Mater., 114 (2008) 387–394.
[17] S.-H. Wu, C.-Y. Mou, H.-P. Lin, Synthesis of mesoporous silica nanoparticles, Chem. Rev. Soc., 42 (2013) 3862–3875.
[18] H. Setyawan, R. Balgis, Mesoporous silicas prepared from sodium silicate using gelatin templating, Asia-Pac. J. Chem. Eng., 7 (2012) 448–454.
[19] U. Kalapathy, A. Proctor, J. Shultz, A simple method for production of pure silica from rice hull ash, Bioresour. Technol., 73 (2000) 257–262.
[20] S. Noor, H. Rohasliney, Rice husk as biosorbent: a review, Health Environ. J., 3 (2012) 89–95.
[21] Y. Chen, S.-R. Zhai, N. Liu, Y. Song, Q.-D. An, X.-W. Song, Dye removal of activated carbons prepared from NaOH-pretreated rice husks by low-temperature solution-processed carbonization and H_3PO_4 activation, Bioresour. Technol., 144 (2013) 401–409.
[22] L. Lin, S.-R. Zhai, Z.-Y. Xiao, Y. Song, Q.-D. An, X.-W. Song, Dye adsorption of mesoporous activated carbons produced from NaOH-pretreated rice husks, Bioresour. Technol., 136 (2013) 437–443.
[23] A. Cheenmatchaya, S. Kungwankunakorn, Preparation of activated carbon derived from rice husk by simple carbonization and chemical activation for using as gasoline adsorbent, Int. J. Environ. Sci. Dev., 5 (2014) 171–175.
[24] M.S. Balathanigaimani, H.-C. Kang, W.-G. Shim, C. Kim, J.-W. Lee, H. Moon, Preparation of powdered activated carbon from rice husk and its methane adsorption properties, Korean J. Chem. Eng., 23 (2006) 663–668.
[25] X. He, P. Ling, M. Yu, X. Wang, X. Zhang, M. Zheng, Rice husk-derived porous carbons with high capacitance by $ZnCl_2$ activation for supercapacitors, Electrochim. Acta, 105 (2013) 635–641.
[26] M.S. Masoud, W.M. El-Saraf, A.M. Abdel-Halim, A.E. Ali, E.A. Mohamed, H.M.I. Hasan, Rice husk and activated carbon for waste water treatment of El-Mex Bay, Alexandria Coast, Egypt, Arabian J. Chem., 9 (2016) S1590–S1596.
[27] R. Ghosh, S. Bhattacherjee, A review study on precipitated silica and activated carbon from rice husk, J. Chem. Eng. Process Technol., 4 (2013) 156.
[28] X. Ma, B. Zhou, W. Gao, Y. Qu, L. Wang, Z. Wang, Y. Zhu, A recyclable method for production of pure silica from rice hull ash, Power Technol., 217 (2012) 497–501.
[29] M.S. Hernández, C.S. Hernández, A.G. Fuentes, E. Elorza, M. Carrera-Rodríguez, M.J. Puy Alquiza, Silica from rice husks employed as drug delivery for folic acid, J. Sol-Gel Sci. Technol., 71 (2014) 514–521.
[30] S.M. Mehdinia, K. Moeinian, T. Rastgoo, Rice husk silica adsorbent for removal of hexavalent chromium pollution from aquatic solutions, Iran. J. Energy Environ., 5 (2014) 218–223.
[31] D. Sivakumar, Hexavalent chromium removal in a tannery industry wastewater using rice husk silica, Global J. Environ. Sci. Manage., 1 (2015) 27–40.
[32] K.Y. Foo, B.H. Hameed, Insights into the modeling of adsorption isotherm systems, Chem. Eng. J., 156 (2010) 2–10.
[33] M. Li, M.-y. Li, C.-g. Feng, Q.-x. Zeng, Preparation and characterization of multi-carboxyl-functionalized silica gel for removal of Cu(II), Cd(II), Ni(II) and Zn(II) from aqueous solution, Appl. Surf. Sci., 314 (2014) 1063–1069.
[34] Z. Hu, X. Zhang, D. Zhang, J.-x. Wang, Adsorption of Cu^{2+} on amine-functionalized mesoporous silica brackets, Water Air Soil Pollut., 223 (2012) 2743–2749.
[35] O. Abdelwahab, N.K. Amin, Adsorption of phenol from aqueous solutions by *Luffa cylindrica* fibers: kinetics, isotherm and thermodynamic studies, Eqypt. J. Aquat. Res., 39 (2013) 215–223.
[36] J.A.H. Maldonado, F.A. Torres García, M.M. Salazar Hernández, R. Hernández Soto, Removal of chromium from contaminated liquid effluents using natural brushite obtained from bovine bone, Desal. Wat. Treat., 95 (2017) 262–273.